

## NOTES

## Extended-Chain Crystals of High-Pressure Crystallized Poly(ethylene terephthalate)

Liangbin LI,<sup>\*,\*\*\*,†</sup> Rui HUANG,<sup>\*</sup> Ling ZHANG,<sup>\*</sup> and Shiming HONG<sup>\*\*</sup>

<sup>\*</sup>Department of Polymer Materials Science and Engineering, Sichuan University, Chengdu 610065, P. R. China

<sup>\*\*</sup>Institute of Atomic and Molecular Physics, Sichuan University, Chengdu 610065, P. R. China

<sup>\*\*\*</sup>FOM-Institute of Atomic and Molecular Physics, Kruislaan 407, 1098 SJ Amsterdam, The Netherlands

(Received December 20, 2000; Accepted May 1, 2001)

KEY WORDS     High Pressure / Extended-Chain Crystals / Poly(ethylene terephthalate) /

In previous papers,<sup>1,2</sup> we reported that poly(ethylene terephthalate) (PET) extended-chain crystals could be formed at high pressure, based on the evidence of infrared spectrum (IR), differential scanning calorimetry (DSC) and scanning electron microscopy (SEM). However, it is difficult to observe parallel striation, which is the most common feature of polymer extended-chain crystals,<sup>3</sup> with SEM. Similar phenomenon was also found in other high-pressure crystallized polymers, such as polyethylene (PE)<sup>4,5</sup> and polyamide (PA).<sup>6,7</sup> The morphology of PET extended-chain crystals was only observed in some small regions on the fracture surface of PET samples. This induced a doubt that samples maybe contained small part of extended-chain crystals and most folded-chain crystals. Although the doubt was eliminated by the result of DSC and IR, direct evidence from SEM is also necessary to support the results.

To present a more concrete evidence of the formation of PET extended-chain crystals, we chose PET material with a higher average molecular weight (compared with those used in previous papers) as the original materials. SEM measurements showed that the parallel striated extended-chain crystals of PET distributed all over the fracture surface. The mechanism about fracture of extended-chain crystallized PET samples is discussed based on the SEM results.

### EXPERIMENTAL

An unoriented commercial PET (Yanshan Petrol. Chem. Co. China) was used as the original material. The molecular weight, calculated from viscosity, was about 26000. Before high-pressure treatment, the original PET material was allowed to stand for 36 h at 368 K in vacuum to eliminate moisture. High-pressure experiments were carried out with a piston-cylinder high-pressure apparatus.<sup>8</sup> The following procedure for crystallization was used. After loading the sample, low pressure (30 MPa) was applied and temperature was raised to predetermined level. After equilibrium was established, pressure was raised to a predetermined level. The samples were kept under these conditions for 6 h, and then quenched to ambient condition. This procedure ensured that the polymer temperature would not exceed the crystallization temperature so as to minimize degradation of PET at elevated temperature and also to ensure that the polymer would be molten state before crystallization takes place. The crystallization conditions were listed in Table I.

Calorimetric measurements were performed at atmospheric pressure by using a Perkin–Elmer DSC-2 instrument. The calorimeter was calibrated with standard substance, which melt in the range of PET. The heating rate was 10 K min<sup>-1</sup>. The crystallinity was calculated with the following equation:

**Table I.** High-pressure crystallization conditions and results

Sample	Crystallization conditions	Melting temperature/K	Melting enthalpy/J g <sup>-1</sup>	Crystallinity/%
PET1	300 MPa 603 K 6 h	563.37	100.3	71.7
PET2	300 MPa 623 K 6 h	563.42	121.9	87.1
PET3	250 MPa 623 K 6 h	562.87	94.5	67.5

<sup>†</sup>To whom correspondence should be addressed (E-mail: liangbin@mailsv.amolf.nl).

$$X_c = \Delta H_m / \Delta H_m^0 \quad (1)$$

where  $\Delta H_m^0$  is the equilibrium melting enthalpy, which was  $140 \text{ J g}^{-1}$  suggested by Wunderlich.<sup>9</sup>

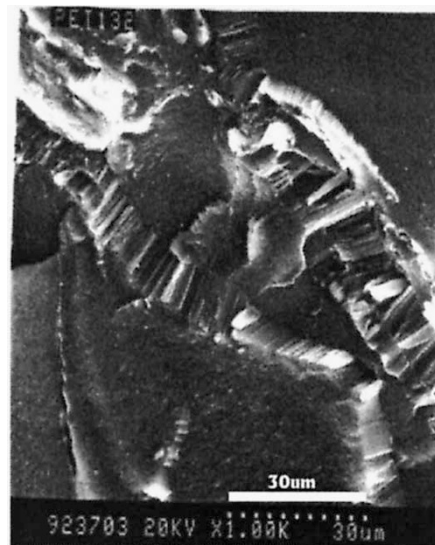
SEM was carried out on a AMRAY 1845FM apparatus. Fracture of specimens was carried out at liquid  $\text{N}_2$  temperature. Before SEM observation, the fracture surfaces were coated with Au. Wide-angle X-Ray diffraction (WAXD) was obtained at room temperature with a D/max-1-a instrument.

## RESULTS AND DISCUSSION

WAXD measurements of these high-pressure crystallized PET samples showed that all diffraction lines corresponded to triclinic structure, which was the same as at atmospheric pressure.<sup>10</sup> This indicated that not any new crystal form was crystallized at high pressure.

The melting temperature ( $T_m$ ), melting enthalpy ( $\Delta H_m$ ) and crystallinity ( $X_c$ ) of these PET samples, obtained with DSC, are listed in Table I. Although the crystallization conditions were different, the melting temperatures of PET1–3 had little difference. They were about 563 K, which were 32 K higher than that of the original material (about 531 K). This suggested that extended-chain crystals of PET were possibly obtained in PET1–3. The crystallinity of PET3 was lower than that of PET1 and 2. In addition to the effect of supercooling and pressure, high-temperature degradation was also an important factor to decrease crystallinity, which commonly occurs at high temperature in polyesters.

Figure 1 gives out three secondary electron images (SEI) of the fracture surface of PET2. They are in different amplifications. The most common morphological feature of extended-chain crystals is the parallel striated appearance. The striations run parallel to the molecular chain direction.<sup>3</sup> The morphology of polymer extended-chain crystals was observed all over the fracture surface. This confirmed that extended-chain crystals of PET were formed in PET2. The distribution of PET extended-chain crystals was not confined in a small region. This is the direct evidence to eliminate the doubt about the content of extended-chain crystals in high-pressure crystallized PET samples. SEM was also consistent with above DSC that PET2 had only one melting temperature. The thickness of extended-chain crystals in PET2 was about  $15 \mu\text{m}$ , which was much longer than the average length of molecular chains. SEI showed that the (001) plane of PET crystals was easy to be exposed instead of (100) and (010) planes during fracture. Figure 2 shows the crystal structure of PET for describing conveniently.<sup>10</sup> The  $c$  axis of most extended-chain crystals was perpendicular to the fracture surface.



(a)



(b)



(c)

**Figure 1.** Secondary electron images of the fracture surface of PET2 crystallized at 300 MPa, 623 K for 6 h.

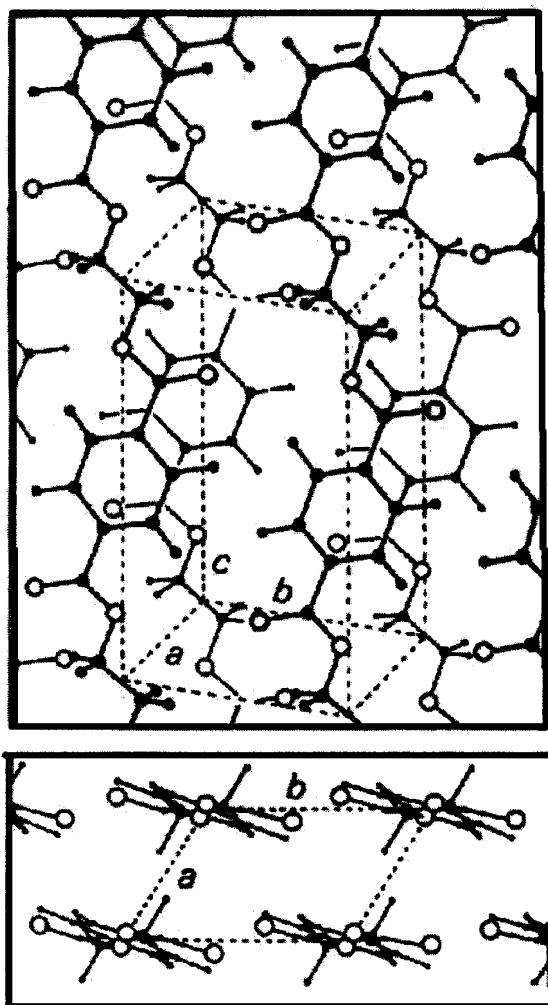


**Figure 2.** Crystal structure of PET.<sup>10</sup>

This suggested that the samples were usually fractured at the interface of lamellar crystals perpendicular to  $c$  axis. When the thickness of lamellar crystals is much longer than the average length of molecular chains, just like that in PET2, there is few tie chain among lamellar crystals along  $c$  axis direction. So the interaction between lamellar crystals at the interface perpendicular to  $c$  axis is very weak and samples are easy to be broken through the interface. Such fracture mechanism prevents (100) and (010) planes from exposing, and hinders us to detect the characteristic morphology of extended-chain crystals of PET. This is a possible reason why some proceeding investigators could not observe the morphology of PET extended-chain crystals with microscopy.<sup>11–13</sup>

SEI of the fracture surface PET3 is shown in Figure 3. The thickness of extended-chain crystals in PET3 was thicker than that in PET2, which was up to 60  $\mu\text{m}$ . However, the melting point of PET3 is lower than that of PET2. This was possibly induced by degradation. High pressure reduces the effect of degradation when samples were treated at same temperature. Accord-

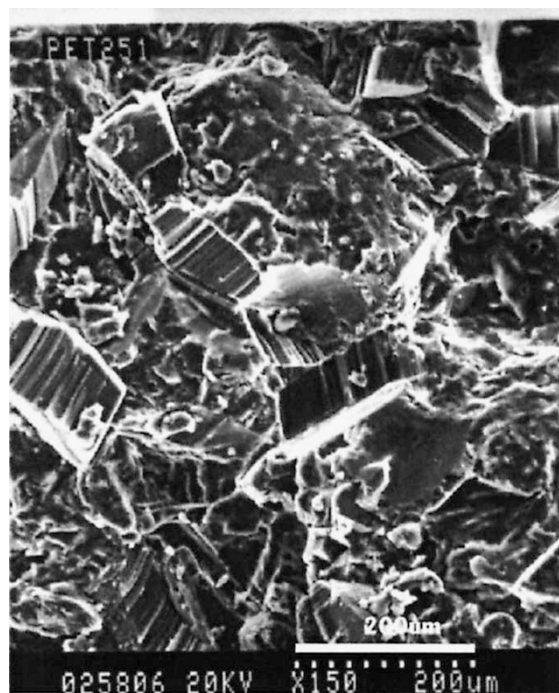


**Figure 3.** Secondary electron image of the fracture surface of PET3 crystallized at 250 MPa, 623 K for 6 h.

ing to the simple Thomason–Gibbs equation,<sup>9</sup> thicker lamellar crystals should correspond to higher melting temperature. Nevertheless, when the thickness is much longer than the length of molecular chains and up to micrometer, the melting temperature of polymer is not controlled significantly by the thickness of lamellar crystals. The most important factor to govern the melting point of polymer should be defects induced by chain ends.<sup>14</sup> So if degradation breaks more molecular chains and produces more chain ends, more defects would exist on the surface and within crystals. This would make the melting temperature of samples decrease obviously, just like the results about PET3.

Although the fractures of PET1 were carried out in different conditions and directions, we could only observe the morphology of spherulites instead of extended-chain crystals with our SEM (amplification less than 12 K). Figure 4 displays a SEI of the spherulite in PET1. Combining the DSC result and SEM observation of PET2 and 3, extended-chain crystals were perhaps also formed in PET1. The failure to expose the striation morphology was possibly due to the small size of extended-chain crystals in PET1. Based on the mechanism for the formation of PET extended-chain crystal,<sup>15</sup> this is also reasonable, because the thickening of PET extended-chain crystals is mainly controlled by transesterification, which is more sensitive to temperature. Interactions between crystalline and amorphous regions, among crystals and within crystals play important roles in the fracture of samples. This result shows

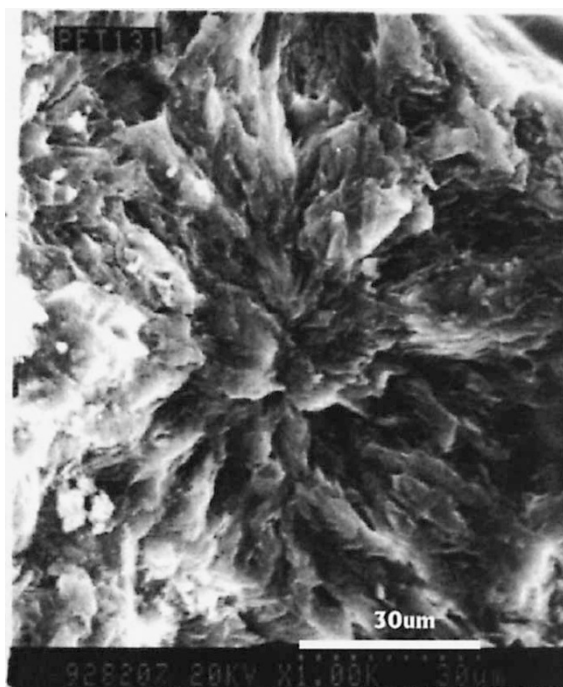


**Figure 4.** Secondary electron image of the fracture surface of PET1 crystallized at 300 MPa, 603 K for 6 h.

that it is difficult to detect the characteristic morphology of PET extended-chain crystals once more.

DSC and SEM results confirmed that PET extended-chain crystals were formed at high pressure. Extended-chain crystals of PET with thickness up to 60  $\mu\text{m}$  were obtained. SEM observation showed that extended-chain crystals distributed all over the high-pressure PET sample instead of confined within a small region. High-pressure crystallized PET samples were readily fractured at the interface of lamellar crystals perpendicular to  $c$  axis, which displayed the (001) plane and

prevented the (100) and (010) planes from exposing.

*Acknowledgments.* The authors gratefully acknowledge the National Science Foundation Financial support, as well as that of the Ministry of Education foundation. The authors extend their gratitude to professors Fu Qiang and Shen Jingwei for helpful discussion.

## REFERENCES

1. L. B. Li, R. Huang, and A. Lu, *Polymer*, **41**, 6943 (2000).
2. L. B. Li, L. Zhang, and R. Huang, *J. Polym. Sci., Part B: Polym. Phys.*, **38**, 1612 (2000).
3. B. Wunderlich, "Macromolecular Physics", Academic Press, Inc., New York, N.Y., 1970, vol. 1, pp 217–231.
4. D. C. Bassett, *Polymer*, **17**, 410 (1976).
5. D. C. Bassett, "Principles of Polymer Morphology", Cambridge University Press, New York, N.Y., 1980.
6. S. Gogolewski and A. J. Pennings, *Polymer*, **18**, 654 (1977).
7. S. Gogolewski and A. J. Pennings, *Polymer*, **18**, 667 (1977).
8. Q. Fu, R. Huang, and X. W. Zhang, *Sci. China*, **A24**, 1218 (1994).
9. B. Wunderlich, "Macromolecular Physics", Academic Press, Inc., New York, N.Y., 1980, vol. 3, pp 225.
10. R. D. Daubery, C. W. Bunn, and C. J. Brown, *Proc. R. Soc. London, Ser. A*, **226**, 531 (1954).
11. N. Hiramatsu and S. Hirakawa, *Polym. J.*, **12**, 105 (1980).
12. C. M. Roland, *Polym. Eng. Sci.*, **31**, 849 (1991).
13. Y. Kitano, Y. Kinoshito, and T. Ashida, *Polymer*, **36**, 1947 (1995).
14. L. B. Li, R. Huang, C. M. Wang, L. Zhang, S. M. Hong, and Q. Fu, *J. Macromol. Sci., Phys. B* (in press).
15. L. B. Li, R. Huang, L. Zhang, and S. M. Hong, *Polymer*, **42**, 2085 (2001).